Romanian Reports in Physics, Vol. 58, No. 3, P. 319–324, 2006

NUMERICAL SCHEMES FOR LATTICE BOLTZMANN MODELS

ARTUR CRISTEA

Laboratory for Numerical Simulations and Parallel Computing for Fluid Mechanics,
Center for Fundamental and Advanced Technical Research, Romanian Academy,
Bd. Mihai Viteazul 24, 300223, Timisoara
Email: f1astra@acad-tim.tm.edu.ro

(Received March 14, 2006)

Abstract. TVD and flux limiter numerical schemes are used to improve the accuracy of the simulation results for a isothermal lattice Boltzmann model for liquid – vapour fluid systems.

Key words: isothermal lattice Boltzmann, finite difference schemes, spurious behaviour.

1. INTRODUCTION

Lattice Boltzmann (LB) models [1,2,3,4,5] provide an alternative to current methods in computational fluid dynamics (CFD). Unlike conventional numerical techniques based on the discretization of the macroscopic fluid equations, LB models are based on the physics at the mesoscopic scale, while the macroscopic level phenomena are recovered from evolution equations which contain the force $\mathbf{F} = m\mathbf{a}$ acting on a fluid particle of mass m. Due to their local nature, LB models are suitable for parallel computing.

The starting point of LB models is the set of evolution equations for the distribution functions $f_i(\mathbf{x},t)$, which is recovered from the Boltzmann equation after discretisation of the phase space [6]:

$$\partial_t f_i(\boldsymbol{x},t) + \boldsymbol{e}_i \cdot \nabla f_i(\boldsymbol{x},t) = -\frac{1}{\tau}[f_i(\boldsymbol{x},t) - f_i^{eq}(\boldsymbol{x},t)] + \frac{1}{k_B T}\boldsymbol{F}\cdot[\boldsymbol{e}_i - \boldsymbol{u}(\boldsymbol{x},t)]f_i^{eq} \qquad (1)$$
$$i = 0,1,...\mathrm{N}$$

Here $\{\mathbf{e}_i\}$ is the discrete set of particle velocities, while position vectors $\mathbf{x}$ belong to a discrete lattice L. For an isothermal LB model in the 1D case (N=2) we have:

$$\boldsymbol{e}_i = \begin{cases} 0 & , \quad i = 0 \\ c & , \quad i = 1 \\ -c & , \quad i = 2 \end{cases} \qquad (2)$$

where $c = \sqrt{\frac{k_B T}{\chi m}}$ is the thermal speed (k_B is the Boltzmann constant, T is the temperature of the system and $\chi = 1/3$).

The equilibrium distribution functions f_i^{eq} are expressed as a series expansion in the local velocity $\boldsymbol{u} = \boldsymbol{u}(\boldsymbol{x}, t)$:

$$f_i^{eq}(\mathbf{x}, t) = w_i n\left[1 + \frac{\mathbf{e}_i \cdot \mathbf{u}}{\chi c^2} + \frac{(\mathbf{e}_i \cdot \mathbf{u})^2}{2\chi^2 c^4} - \frac{\mathbf{u} \cdot \mathbf{u}}{2\chi c^2}\right] \tag{3}$$

The weight factors for the 1D isothermal LB models are: $w_0 = 2/3,\ w_1 = w_2 = 1/6$.

2. THE EVOLUTION EQUATIONS

The non-dimensionalized momentum conservation equation of the model is:

$$\partial_t(\rho\, \boldsymbol{u}) + \nabla(\rho\, \boldsymbol{uu}) = -\nabla p + \nu\nabla(\rho\, \nabla \boldsymbol{u}) + \rho\, \boldsymbol{a} \tag{4}$$

where ρ is the local fluid density and ν is the fluid viscosity. To retrieve a non-ideal equation of state for the pressure $p = p(\rho, T)$, the force term in Eq. (1) should be:

$$\boldsymbol{F} = m\boldsymbol{a} = -\frac{m}{\rho}\nabla(p_w - p_{id}) \tag{5}$$

where the non-dimensionalized Van der Waals pressure p_w [7] and respectively the non-dimensionalized ideal gas pressure p_{id} are:

$$\begin{aligned} p_w &= \frac{3\rho T}{3-\rho} - \frac{9}{8}\frac{\rho^2}{T} \\ p_{id} &= \chi c^2 \rho \end{aligned} \tag{6}$$

With these relations, taking into account the relation $c = \frac{1}{\chi m}$, the equilibrium distribution functions (3) and the surface tension [8], the force term in the LB equation becomes (up to second order in u):

$$\frac{\boldsymbol{F}}{\chi c^2 m}[\boldsymbol{e}_i - \boldsymbol{u}] f_i^{eq} = -\frac{w_i}{m}\left[\frac{\boldsymbol{e}_i - \boldsymbol{u}}{\chi c^2} + \frac{(\boldsymbol{e}_i \cdot \boldsymbol{u})\, \boldsymbol{e}_i}{\chi^2 c^4}\right] \cdot [\nabla(p_w - p_{id}) + 3k\rho(\nabla^2\rho)] \tag{7}$$

3. FINITE DIFFERENCE SCHEMES

The phase space discretized Boltzmann equations (1) may be solved numerically using an appropriate finite difference scheme defined on the lattice. When using a characteristic based finite difference scheme, the forward Euler finite difference is used to compute the time derivative and the distribution functions $f_{i,j}$ are updated at each lattice node j, at time step n+1. Flux limiter techniques [9,10] are currently used to improve the numerical stability of the finite difference schemes. When using a flux limiter technique to compute space derivatives, the left hand-side of Eq. (1) becomes:

$$f_{i,j}^{n+1} - f_{i,j}^{n} + \delta t \boldsymbol{e}_i \cdot (\nabla f_i^{\,n})_j = f_{i,j}^{n+1} - f_{i,j}^{n} + CFL[F_{i,j+1/2}^{n} - F_{i,j-1/2}^{n}] \tag{8}$$

where $CFL = c\delta t / \delta x$ is the Courant-Friedrichs-Levy number and

$$\begin{aligned} F_{i,j+1/2}^{n} &= f_{i,j}^{n} + \frac{1}{2}(1-CFL)\left[f_{i,j+1}^{n} - f_{i,j}^{n} \right] \psi(\theta_{i,j}^{n}) \\ F_{i,j-1/2}^{n} &= f_{i,j-1}^{n} + \frac{1}{2}(1-CFL)\left[f_{i,j}^{n} - f_{i,j-1}^{n} \right] \psi(\theta_{i,j-1}^{n}) \end{aligned} \tag{9}$$

are numerical fluxes. The flux limiter $\psi(\theta_{i,j}^{n})$ is expressed as a function of the *smoothness*:

$$\theta_{i,j}^{n} = \frac{f_{i,j}^{n} - f_{i,j-1}^{n}}{f_{i,j+1}^{n} - f_{i,j}^{n}} \tag{10}$$

Standard finite difference schemes are recovered from Eq. (9) for two particular values of the flux limiters: $\psi(\theta_{i,j}^{n}) = 0$ (upwind scheme) and $\psi(\theta_{i,j}^{n}) = 1$ (Lax Wendroff scheme). In this paper, we will use the Monitorized Central Difference (MCD) flux limiter.

$$\psi(\theta_{i,j}^{n}) = \begin{cases} 0 & , \quad \theta_{i,j}^{n} \le 0 \\ 2\theta_{i,j}^{n} & , \quad 0 \le \theta_{i,j}^{n} < \frac{1}{3} \\ \dfrac{1+\theta_{i,j}^{n}}{2} & , \quad \frac{1}{3} \le \theta_{i,j}^{n} < 3 \\ 2 & , \quad \theta_{i,j}^{n} > 3 \end{cases} \tag{11}$$

The TVD numerical scheme [11,12] starts from the same discretized equation (8), but the expression of the two fluxes is a bit more complicated:

$$F^{n}_{i,j+1/2} = \frac{1}{2c}\left[cf^{n}_{i,j+1} + cf^{n}_{i,j} + g^{n}_{i,j+1} + g^{n}_{i,j} - Q(c+\gamma^{n}_{i,j+1/2})\Delta^{n}_{i,j+1/2}\right] \quad (12)$$

Q(x) is a function that eliminates the so-called entropy violation, and the definition for the function g is recovered using the *Minmod* operation: $g^{n}_{i,j} = Min\,\mathrm{mod}(g^{n}_{i,j+1/2}; g^{n}_{i,j-1/2})$,
where:

$$g^{n}_{i,j+1/2} = \frac{1}{2}(Q(c) - c^2\frac{\delta t}{\delta s})\Delta^{n}_{i,j+1/2} \quad (13)$$

$$\Delta^{n}_{i,j+1/2} = f^{n}_{i,j+1} - f^{n}_{i,j} \quad (14)$$

$$\gamma^{n}_{i,j+1/2} = \begin{cases} (g^{n}_{i,j+1} - g^{n}_{i,j})\Delta^{n}_{i,j+1/2} & ; \quad \Delta^{n}_{i,j+1/2} \neq 0 \\ 0 & ; \quad \Delta^{n}_{i,j+1/2} = 0 \end{cases} \quad (15)$$

4. NUMERICAL RESULTS

The main characteristic of the liquid-vapour systems is the phase separation, which occurs when the system temperature is lowered below the critical temperature $T_c = 1$. In the final state, the existence of two different phases: the liquid phase (with higher density) and the gas phase (with lower density) can be seen (Fig. 1a). The results we get using the TVD schemes are closer to the theoretical diagram derived from the *Maxwell construction* [7]. When using the UPWIND scheme, a *spurious* velocity (Fig. 1b) is observed in the interface region. These features are strongly reduced when using the MCD / TVD schemes.

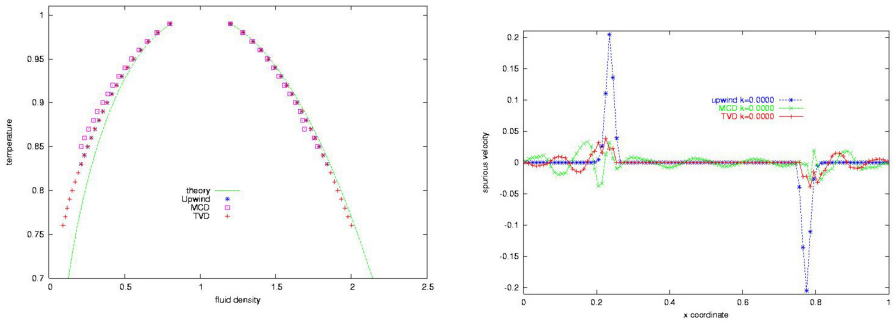

a. b.

Fig. 1 – Phase diagram for liquid-vapour systems(a); Spurious velocities (b).

The unphysical behaviour of the liquid-vapour system appears because of a spurious term [13] in the continuity equation (13):

$$\partial_t \rho + \nabla\left[\rho \boldsymbol{u} - \frac{1}{2}\chi c \delta x \nabla \rho\right] = 0 \tag{16}$$

The spurious term acts in the interface region, where large density gradients are present.

The introduction of a nonzero surface tension in the force term improves the numerical results, being useful both for the first order UPWIND scheme and the MCD / TVD high order schemes (Figs. 2a; 2b). The computed phase diagram become closer to the theoretical one and the spurious velocities are strongly reduced, in the interface region.

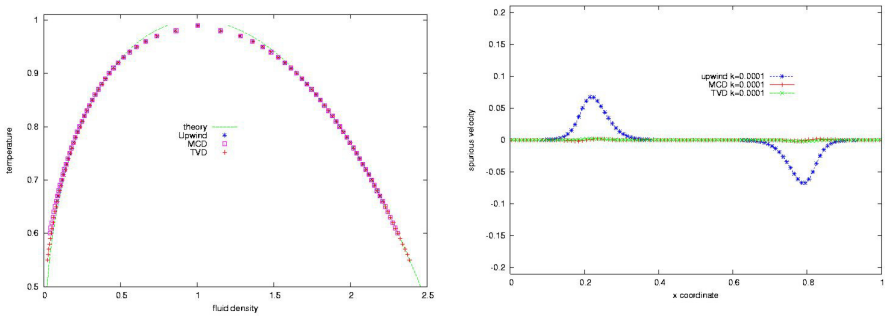

a. b.

Fig. 2 – Phase diagram for liquid-vapour systems (surface tension parameter k = 0.0001) (a); Spurious velocities (surface tension parameter k = 0.0001) (b).

5. CONCLUSIONS

In this paper we discuss the spurious effects, introduced by the numerical schemes used in a finite difference isothermal lattice Boltzmann model for the simulation of liquid-vapour systems. Phase separation is achieved through an interparticle force. The choice of an appropriate numerical scheme is essential to reduce the spurious behaviour in the interface region.

Acknowledgements. This work was supported partially by the Romanian Ministry of Research (MEC) under CEEX Programme (Project PC-D01-PT04-257 Contract 11/2005-2008) and by CINECA under Project HPC-EUROPA (RII3-CT-2003-506079), with the support of the European Community – Research Infrastructure Action under FP6 Structuring the European Research Area Programme [14,15]. A parallel computer code for isothermal LB model was implemented using PETSc 2.2.1 (Portable Extensible Toolkit for Scientific Computation) developed at the Argonne National Laboratory, Argonne, Illinois [16].

REFERENCES

1. D.H. Rothmann, S. Zaleski, *Lattice – Gas Cellular Automata, Simple Models of Complex Hydrodynamics*, Cambridge, Cambridge University Press, 1997.
2. S. Chen, G.D. Doolen, *Lattice – Boltzmann Method for Fluid Flows*, Annual Review of Fluid Mechanics 30, 1998, p. 329.
3. B. Chopard, M. Droz, *Cellular Automata Modelling of Physical Systems*, Cambridge, Cambridge University Press, 1998.
4. D.A. Wolf – Gladrow, *Lattice – Gas Cellular Automata and Lattice – Boltzmann Models*, Berlin, Springer Verlag, 2000.
5. S. Succi, *The Lattice Boltzmann Equation for Fluid Dynamics and Beyond*, Oxford, Oxford University Press, 2001.
6. L.S. Luo, Physical Review E **62**, 2000, p. 4982.
7. D. Kondepudi, I. Prigogine, *Modern Thermodynamics: From Heat Engines to Dissipative Structures*, Chichester, New York, John Willey & Sons, 1998.
8. A. Cristea, V. Sofonea, International Journal of Modern Physics C **14**, 2003, p.1251.
9. R.J. LeVeque, *Numerical Methods for Conservation Laws*, Basel, Birkhauser Verlag, 1992.
10. E.F. Toro, *Riemann Solvers and Numerical Methods for Fluid Dynamics*, Berlin, Springer Verlag, 1999.
11. Y.Chen, S. Teng, T. Shukuwa, H. Ohashi, International Journal of Modern Physics C **9**, 1998, p. 1383.
12. S. Teng, Y. Chen, H. Ohashi, Int. Journal of Heat and Fluid Flow **21**, 2000, p. 112.
13. V. Sofonea, R.F. Sekerka, Journal of Computational Physics **184**, 2003, p.422.
14. Cineca: www.cineca.it/
15. HPC-EUROPA: www.hpc-europa.org/
16. S. Balay, K. Buskelman, V. Eijkhout, W.D. Gropp, D. Kaushik, M. Knepley, L.C. McInnes, B.F. Smith, H. Zhang, *PETSc User's Manual,* Argonne National Laboratory ANL–95/11, Revision 2.2.1, August18, 2004, www-unix.mcs.anl.gov/petsc/petsc-as/index.html